JACS
JOURNAL OF THE AMERICAN CHEMICAL SOCIETY
Communication
pubs.acs.org/JACS

Identification of Fumarate Hydratase Inhibitors with Nutrient-Dependent Cytotoxicity

Toshifumi Takeuchi,[†] Paul T. Schumacker,[§] and Sergey A. Kozmin*[,†]

[†]Department of Chemistry, University of Chicago, Chicago, Illinois 60637, United States
[§]Department of Pediatrics, Division of Neonatology, Feinberg School of Medicine, Chicago, Illinois 60611, United States

Supporting Information

ABSTRACT: Development of cell-permeable small molecules that target enzymes involved in energy metabolism remains important yet challenging. We describe here the discovery of a new class of compounds with a nutrient-dependent cytotoxicity profile that arises from pharmacological inhibition of fumarate hydratase (also known as fumarase). This finding was enabled by a high-throughput screen of a diverse chemical library in a panel of human cancer cell lines cultured under different growth conditions, followed by subsequent structure−activity optimization and target identification. While the highest cytotoxicity was observed under low glucose concentrations, the antiproliferative activities and inhibition of oxygen consumption rates in cells were distinctly different from those displayed by typical inhibitors of mitochondrial oxidative phosphorylation. The use of a photoaffinity labeling strategy identified fumarate hydratase as the principal pharmacological target. Final biochemical studies confirmed dose-dependent, competitive inhibition of this enzyme *in vitro*, which was fully consistent with the initially observed growth inhibitory activity. Our work demonstrates how the phenotypic observations combined with a successful target identification strategy can yield a useful class of pharmacological inhibitors of an enzyme involved in the operation of tricarboxylic acid cycle.

Glycolysis, tricarboxylic acid (TCA) cycle and oxidative phosphorylation (OXPHOS) are the three main components of eukaryotic energy metabolism. The ability to pharmacologically modulate individual biochemical steps of such pathways using cell-permeable small molecules provides new avenues for research in human biology and drug discovery. Many highly effective pharmacological modulators of OXPHOS have been identified over the years.[1−3] Such compounds have been particularly valuable in elucidating and studying the electron-transport chain (ETC) of mitochondria.[4] In contrast, there is only a limited arsenal of potent and selective small-molecule modulators of enzymes involved in glycolysis and TCA cycle. We have previously reported a simple and effective strategy for identification of inhibitors of glycolysis, which was enabled by the ability of such compounds to block ATP production in human cells with chemically impaired mitochondria.[5] We describe here the discovery of a new class of compounds with a highly characteristic nutrient-dependent cytotoxicity that arises from pharmacological inhibition of fumarate hydratase, an enzyme of the TCA cycle.

We screened a collection of nearly 6000 small molecules in several human cancer cell lines under different growth conditions. The chemical library was assembled over a number of years by a series of parallel synthetic strategies and incorporated over 40 different drug-like heterocycles.[6−8] In addition to high level of structural diversity, this compound collection also featured favorable physicochemical properties, including molecular weight, lipophilicity, polar surface area as well as numbers of rotatable bonds and hydrogen-bond donors and acceptors. In the course of this study, we found that pyrrolidinone **1** (Figure 1A) elicited a nutrient-dependent

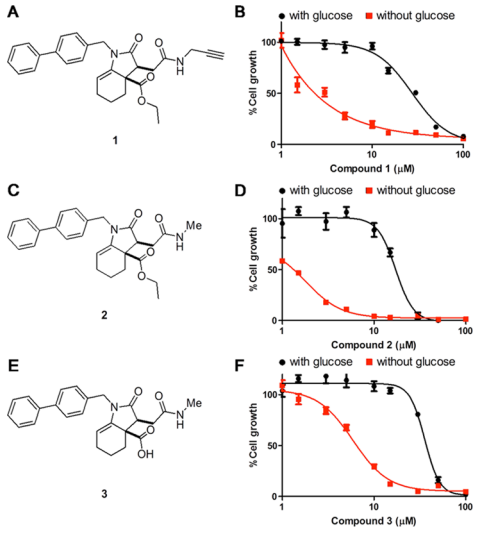

Figure 1. Structure and effects of compounds **1**−**3** on growth of SW620 cell line cultured in DME medium with or without glucose. Each value is a mean ± SEM of triplicate values from three independent experiments.

cytotoxicity in a number of cancer cell lines. For example, compound **1** displayed increased growth-inhibitory activity toward SW620 cell line grown in the absence of glucose, while a substantially lower activity was observed using a standard glucose-containing Dulbecco's Modified Eagle's (DME) medium (Figure 1B). In search for more selective and potent pharmacological agents, we next constructed a focused library of

Received: October 1, 2014
Published: December 3, 2014

DOI: 10.1021/ja5101257
J. Am. Chem. Soc. 2015, 137, 564−567

structural analogs of pyrrolidinone **1** (Figure S1). The design of a secondary library was guided by the structure−activity data from the primary screen of the original library, which incorporated a number of derivatives of **1** with both peripheral and core alterations. We found that truncation of propargyl moiety to a methyl group was beneficial. The resulting pyrrolidinone **2** (Figure 1C) demonstrated not only an increase in cell-growth inhibitory activity against SW620 cell line but also an enhanced selectivity (Figure 1D). Replacing propargyl group with larger substituents abolished both the activity and selectivity of the resulting compounds (Figure S1). Conversion of the ethyl ester **2** to the corresponding carboxylic acid **3** (Figure 1E) was tolerated albeit with a slightly diminished activity but a similar nutrient dependence on its antiproliferative activity (Figure 1F). We also established that this class of compounds was configurationally stable at pH 6−8 (Figure S11).

We next examined the generality of the observed nutrient dependence on the activity of this class of compounds in a number of histologically different cancer cell lines, which were grown in standard DME medium or in L-15 medium.[9] Representative dose-dependent activity data for the most potent compound **2** in five representative cell lines cultured in the absence of glucose are shown in Figure 2A. All cell lines were

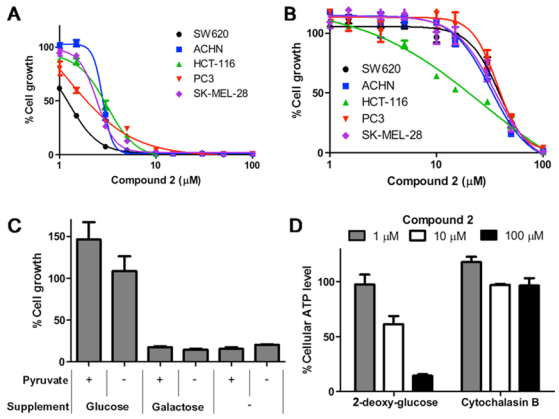

Figure 2. Effects of compound **2** on growth of human cancer cell lines under different conditions. (A) Antiproliferative activities of compound **2** on SW620, ACHN, HCT-116, PC3, and SK-MEL-28 cells cultured in L-15 medium. (B) Antiproliferative activities of compound **2** on SW620, ACHN, HCT-116, PC3, and SK-MEL-28 cells cultured in DME medium. (C) Effect of compound **2** on proliferation of SW620 cells after 48 h under several different growth conditions using glucose-free DME medium supplemented with glucose (2 mM), galactose (2 mM), or sodium pyruvate (1 mM). (D) Cellar ATP levels in SW620 cells after rapid (30 min) exposure to compound **2** and glycolysis inhibitors, including 2-deoxy-glucose (10 mM) or cytochalasin B (10 μM). Each value is a mean ± SEM of triplicate values from three independent experiments.

found to be highly sensitive to this agent with a mean IC_{50} of 2.2 μM. When the same cell lines were grown in the presence of glucose, the growth inhibitory activity of **2** was diminished more than 10-fold (Figure 2B). Furthermore, replacing glucose with galactose or pyruvate resulted in substantially lower survival of SW620 cells that were grown under such alternative carbon sources in the presence of compound **2** (Figures 2C and S2). Such observations strongly suggested that compounds **1**−**3** might exert their effects on a mitochondrial target since the activity of this organelle would be required for survival if glycolysis was suppressed.[10,11] We next examined the effect of compound **2** on ATP production in SW620 cells in the presence of known glycolytic inhibitors.[5] We found that ATP concentration was rapidly (within 30 min) decreased by **2** in dose-dependent manner in the presence of 10 mM concentration of 2-deoxyglucose (Figure 2D). However, compound **2** did not block ATP production in SW620 cells in the presence of cytochalasin B (Figure 2D) or other glucose transport inhibitors (Figure S3). The latter effect was distinctly different from that displayed by OXPHOS inhibitors, which blocked ATP production in cells treated with glucose transport inhibitors.[5] Furthermore, while NADH levels typically rapidly rise in cells treated with OXPHOS inhibitors,[12] such effects were not observed for any of the compounds **2** and **3** (Figure S4), suggesting that they did not block mitochondrial ETC or ATP synthase.

We next examined the effects of newly identified compounds on cellular respiration. While inhibition of both OXPHOS and TCA cycle may impair oxygen consumption rate (OCR), such studies can be used to clearly distinguish between such effects on cells. We first analyzed OCR of SW620 cells treated with the most potent compound **2** at several concentrations in the range of 0.5−5.0 μM. As shown in Figure 3A, the respiration rate was

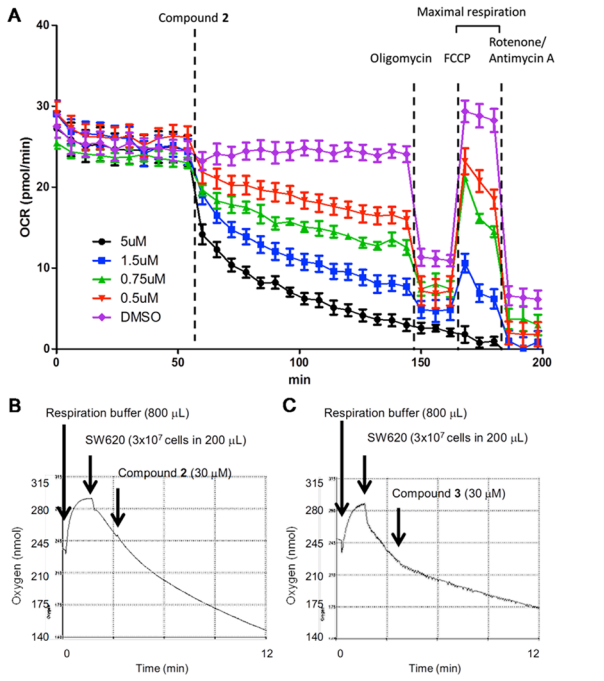

Figure 3. Effects of compounds **2** and **3** on cellular respiration. (A) Real-time measurement of OCR in SW620 cells treated with several concentrations of compound 2 (0, 0.5, 0.75, 1.5, 5 μM). OCR was measured using XFe96 analyzer. Positive controls included oligomycin (1 μM), FCCP (0.5 μM), and rotenone (1 μM)/antimycin A (1 μM) mixture. Error bars indicate standard errors. (B) Real-time measurement of oxygen consumption using Clark-type oxygen electrode of SW620 cells treated with compound **2**. (C) Real-time measurement of oxygen consumption using Clark-type oxygen electrode of SW620 cells treated with compound **3**.

reduced in a dose-dependent manner. At the highest concentration tested, compound **2** blocked cellular respiration in SW620 cells completely. This effect could not be rescued by a proton uncoupling agent, such as carbonyl cyanide-4-(trifluoromethoxy)-phenylhydrazone (FCCP), which clearly established that **2** did not inhibit ATP synthase. Since it appeared that OCR was reduced by **2** gradually within the first 30 min of treatment of

DOI: 10.1021/ja5101257
J. Am. Chem. Soc. 2015, 137, 564−567

cells, we next used Clark-type oxygen electrode to analyze the kinetics of this effect.[13] This study confirmed that pyrrolidinone **2** slowly and gradually reduced cellular respiration of SW620 cells (Figures 3B and S5). Further experiments demonstrated that while cellular respiration was inhibited by either **2** or rotenone, the respiration was reinitiated by succinate, indicating that **2** did not inhibit complex II–IV activities (Figures S5 and S6).[14] We further established that **2** did not have any effects on activity of complex I of ETC using submitochondrial particles generated from SW620 cells (Figure S7). These studies conclusively demonstrated that compound **2** did not directly block any of the complexes of mitochondrial ETC and its effect may therefore arise from blocking the TCA cycle. Such inhibitory activity would be expected to impair cellular respiration.[15]

We also used Clark-type oxygen electrode to examine the effects of carboxylic acid **3** on cellular respiration in the same cell line. Interestingly, the oxygen consumption was reduced immediately upon treatment of cells with **3** (Figures 3C and S8) with the same overall profile displayed by **2**. The difference in the kinetics of cellular respiration inhibition suggested that ester **2** might be hydrolyzed in the cell to acid **3**, serving as a pro-drug with an increased cellular permeability.[16] Indeed, a detailed LC-MS analysis confirmed the presence of carboxylic acid **3** in the extracts of SW620 cells treated with ester **2** (Figures S9 and S10). We further demonstrated that **3** did not have any effects on activity of any of the complexes of mitochondrial ETC (Figures S8 and S12).

To identify the cellular target of this compound class, we generated a chemical probe **4** armed with a benzophenone group and an alkyne tag (Figure 4A). The benzophenone group, which replaced a biphenyl moiety of the initial compounds, was designed for covalent photoaffinity labeling of the cellular target.[17,18] The alkyne moiety would facilitate identification of the photo-cross-linked proteins.[19] Compound **4** displayed similar activity profile to that observed for the initial set of compounds **1**–**3**, indicating that the benzophenone group and the terminal alkyne were well tolerated (Figure S13). We also prepared a closely related negative control **5** (Figure 4B), which showed no biological activity (Figure S13). The photoaffinity labeling experiments were carried out with SW620 cells. Cells were treated with photoaffinity probe **4**, followed by irradiation at 365 nm, lysis of cells, and labeling of any alkyne-containing proteins with azide-conjugated Alexa Fluor 488 dye using Cu-catalyzed azyde-alkyne cycloaddition.[20] The proteins were analyzed by SDS-PAGE and visualized by in-gel fluorescence scanning.

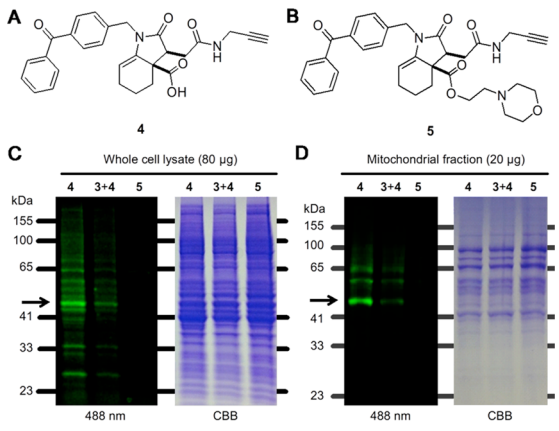

Figure 4. Target identification by photoaffinity labeling. (A, B) Structures of probes **4** and **5**, which were used for photoaffinity labeling of binding proteins in SW620 cells. The cells were treated with either of the above probe **4** (5 μM) or **5** (5 μM) in the absence or presence of **3** (10 μM), irradiated at 365 nm and lysed. Photocrossslinked proteins were next labeled with azide-conjugated Alexa Fluor 488 and analyzed by SDS-PAGE. (C) Fluorescence imaging and coomassie brilliant blue (CBB) staining of SDS-PAGE separated proteins from whole SW620 cell lysate following treatment with photoaffinity probes, UV irradiation and fluorescent dye labeling. (D) Fluorescence imaging and CBB staining of SDS-PAGE separated proteins from mitochondrial fraction of SW620 cells following treatment with photoaffinity probes, UV irradiation, and fluorescent dye labeling.

The results of such experiments using whole cell extract and the mitochondrial fraction are shown in Figure 4C,D, respectively. In both cases, the use of a photoaffinity probe **4** resulted in the appearance of a major protein band at 50 kDa. Similar studies using negative control **5** did not produce the same result, indicating that the 50 kDa protein may be the cellular target of this compound class. Photoaffinity labeling experiments using probe **4** following treatment of cells with compound **3** reduced the intensity of the 50 kDa band, further supporting the evidence that the 50 kDa protein was a high affinity binding protein (Figure S15). Excision of the 50 kDa band, followed by in-gel digestion and LC-MS analysis, unambigiuously established this protein as fumarate hydratase (Table S1 and S2), which is known to reside in mitochondria[21] and serve as a component of the TCA cycle. Indeed, confocal fluorescence microscopy studies confirmed localization of probes **1** and **4** in mitochondria of SW620 cells (Figure S15). We also performed similar photo-affinity labeling experiments with the ester-containing derivative of **4** (Figure S14), which revealed Hsp70 and fumarate hydratase as the two main protein bands (Table S3). Identification to Hsp70 is likely not functionally significant and may simply represent binding of a more lipophilic small molecule to this protein. Appearance of the fumarate hydratase band, however, is consistent with hydrolysis of the ester prior to protein cross-linking.

We next carried out *in vitro* fumarate hydratase activity assays. The activity of this enzyme was measured using a well-established assay that monitored the conversion of fumarate into L-malate and subsequent oxidation of L-malate to oxaloacetate by malate dehydrogenase (Scheme S1). Initial controls established that neither the carboxylic acid **3** nor ester **2** inhibited malate dehydrogenase (Figure S16B). Using this two-enzyme protocol we found that carboxylic acid **3** inhibited fumarate hydratase in a dose-dependent fashion *in vitro* (Figure 5A). However, ester **2** did not exert such effects on this enzyme (Figure S16A), further supporting the evidence that this

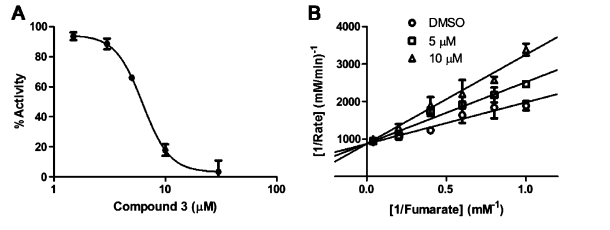

Figure 5. Inhibition of fumarate hydratese with compound **3** *in vitro*. (A) Dose-dependent inhibition of fumarate hydratase, which was isolated from SW620 cells, by compound **3**. (B) Lineweaver–Burk plot of the inhibition of fumarate hydratase by **3**. Kinetic parameters: K_i = 4.5 μM (competitive inhibition), K_m = 1.3 mM, V_{max} =1.1 μM/min.

DOI: 10.1021/ja5101257
J. Am. Chem. Soc. 2015, 137, 564–567

compound served as a pro-drug, being converted into the active inhibitor **2** upon entering the cell. Further experiments established that acid **3** was a competitive inhibitor of fumarate hydratase with a K_i value of 4.5 μM (Figure 5B), which was fully consistent with antiproliferative activity of this compound. Similar experiments were conducted to confirm fumarate hydratase inhibitory activity of compound **4**, which was employed for photoaffinity labeling studies (Figure S18).

In conclusion, we have developed a novel class of cell-permeable inhibitors of fumarate hydratase. This work was enabled by the initial observation of nutrient-dependent cytotoxicity of such compounds, followed by target identification using an effective photoaffinity labeling strategy. Such compounds display an interesting structure−activity profile and provide useful chemical probes for modulating the activity of fumarate hydratase in live cells. Chemical inhibition of fumarate hydratase renders cells highly dependent on glucose metabolism for survival. In the field of cancer biology, recent interest has focused on the identification of genetic disruptions in metabolism that render tumor cells selectively dependent on alternative pathways for survival.[22] Humans carrying mutations in fumarate hydratase are predisposed to the development of leiomyomatosis and renal cancers, in cells that undergo loss of heterozygosity. The increases in fumarate and succinate caused by loss of fumarate hydratase can then promote tumor progression through the activation of the hypoxia-inducible transcription factor.[23−26] Hence, inhibition of fumarate hydratase can contribute to tumorigenicity in some cells. However, many tumor cells exhibit high basal levels of oxidative stress, making them vulnerable to therapies that augment the generation of reactive oxygen species or that undermine endogenous antioxidant mechanisms.[27] In that regard, loss of fumarate hydratase results in the accumulation of fumarate that reacts with reduced glutathione, a critical component of the cellular antioxidant defense system, to form succinated glutathione.[28] Subsequent metabolism by glutathione reductase depletes NADPH, a proximal substrate for the maintenance of cellular redox balance and reductive biosynthesis.[29] Hence, fumarate hydratase inhibition may have therapeutic potential arising from the disruption of cellular redox balance and by promoting absolute dependence on glycolysis.

■ ASSOCIATED CONTENT

Supporting Information

Experimental details and data. This material is available free of charge via the Internet at http://pubs.acs.org.

■ AUTHOR INFORMATION

Corresponding Author

skozmin@uchicago.edu

Notes

The authors declare no competing financial interest.

■ ACKNOWLEDGMENTS

We are grateful for financial support to the National Institutes of Health (P50 GM086145) and the Chicago Biomedical Consortium with support from the Searle Funds at the Chicago Community Trust.

■ REFERENCES

(1) Mitochondrial Bioenergetics. In *Methods in Molecular Biology*; Palmeira, C. M., Moreno, A. J., Eds.; Springer: Berlin, 2012; Vol *810*.

(2) Advances in Mitochondrial Medicine. In *Advances in Experimental Medicine and Biology*; Scatena, R., Bottoni, P., Giardina, B., Eds.; Springer: Berlin, 2012; Vol *942*.

(3) Walters, A. M.; Porter, G. A., Jr.; Brookes, P. S. *Circ. Res.* **2012**, *111*, 1222−1236.

(4) Frezza, C.; Cipolat, S.; Scorrano, L. *Nature Protoc.* **2007**, *2*, 287−295.

(5) Ulanovskaya, O. A.; Cui, J.; Kron, S. J.; Kozmin, S. A. *Chem. Biol.* **2011**, *18*, 222−230.

(6) Cui, J.; Matsumoto, K.; Wang, C. Y.; Peter, M. E.; Kozmin, S. A. *ChemBioChem* **2010**, *11*, 1224−1227.

(7) Cui, J.; Hao, J.; Ulanovskaya, O. A.; Dundas, J.; Liang, J.; Kozmin, S. A. *Proc. Natl. Acad. Sci. U.S.A.* **2011**, *17*, 6763−6768.

(8) Lee, H.; Suzuki, M.; Cui, J.; Kozmin, S. A. *J. Org. Chem.* **2010**, *75*, 1756−1759.

(9) Gohil, V. M.; Sheth, S. A.; Nilsson, R.; Wojtovich, A. P.; Lee, J. H.; Perocchi, F.; Chen, W.; Clish, C. B.; Ayata, C.; Brookes, P. S.; Mootha, V. K. *Nat. Biotechnol.* **2010**, *28*, 249−255.

(10) Robinson, B. H.; Petrova-Benedict, R.; Buncic, J. R.; Wallace, D. C. *Biochem. Med. Metab. Biol.* **1992**, *48*, 122−126.

(11) Marroquin, L. D.; Hynes, J.; Dykens, J. A.; Jamieson, J. D.; Will, Y. *Toxicol. Sci.* **2007**, *97*, 539−547.

(12) Ulanovskaya, O. A.; Jajic, J.; Suzuki, M.; Sabharwal, S. S.; Schumacker, P. T.; Kron, S. J.; Kozmin, S. A. *Nature Chem. Biol.* **2008**, *4*, 418−424.

(13) Clark, L. C., Jr.; Kaplan, S.; Matthews, E. C.; Edwards, F. K.; Helmsworth, J. A. *J. Thorac. Surg.* **1958**, *36*, 488−496.

(14) Zhang, J.; Nuebel, E.; Wisidagama, D. R. R.; Setoguchi, K.; Hong, J. S.; Van Horn, C. M.; Im am, S. S.; Vergnes, L.; Malone, C. S.; Koehler, C. M.; Teitell, M. A. *Nat. Protoc.* **2012**, *7*, 1068−1085.

(15) Reisch, A. S.; Elpeleg, O. *Methods Cell. Biol.* **2007**, *80*, 199−222.

(16) Rautio, J.; Kumpulainen, H.; Heimbach, T.; Oliyai, R.; Oh, D.; Järvinen, T.; Savolainen, J. *Nature Rev. Drug Discovery* **2008**, *7*, 255−270.

(17) Dorman, G.; Prestwich, G. D. *Biochemistry* **1994**, *33*, 5661−5673.

(18) Vodovozova, E. L. *Biochemistry (Moscow)* **2007**, *72*, 5−26.

(19) Park, J.; Oh, S.; Park, B. *Angew. Chem., Int. Ed.* **2012**, *51*, 5447−5451.

(20) Rostovtsev, V. V.; Green, L. G.; Fokin, V. V.; Sharpless, K. B. *Angew. Chem., Int. Ed.* **2002**, *41*, 2596−2599.

(21) Bowes, T.; Singh, B.; Gupta, R. S. *Histochem. Cell Biol.* **2007**, *127*, 335−346.

(22) Vander Heiden, M. G.; Cantley, L. C.; Thompson, C. B. *Science* **2009**, *324*, 1029−1033.

(23) Pollard, P. J.; Wortham, N. C.; Tomlinson, I. P. M. *Ann. Med.* **2003**, *35*, 632−639.

(24) Alam, N. A.; Rowan, A. J.; Wortham, N. C.; Pollard, P. J.; Mitchell, M.; Tyrer, J. P.; Barclay, E.; Calonje, E.; Manek, S.; Adams, S. J.; Bowers, P. W.; Burrows, N. P.; Charles-Holmes, R.; Cook, L. J.; Daly, B. M.; Ford, G. P.; Fuller, L. C.; Hadfield-Jones, S. E.; Hardwick, N.; Highet, A. S.; Keefe, M.; MacDonald-Hull, S. P.; Potts, E. D. A.; Crone, M.; Wilkinson, S.; Camacho-Martinez, F.; Jablonska, S.; Ratnavel, R.; MacDonald, A.; Mann, R. J.; Grice, K.; Guillet, G.; Lewis-Hones, M. S.; McGrath, H.; Seukeran, D. C.; Morrison, P. J.; Fleming, S.; Rahman, S.; Kelsell, D.; Leigh, I.; Olpin, S.; Tomlinson, I. P. M. *Hum. Mol. Genet.* **2003**, *12*, 1241−1252.

(25) Pollard, P. J.; Brière, J. J.; Alam, N. A.; Barwell, J.; Barclay, E.; Wortham, N. C.; Hunt, T.; Mitchell, M.; Olpin, S.; Moat, S. J.; Hargreaves, I. P.; Heales, S. J.; Chung, Y. L.; Griffiths, J. R.; Dalgleish, A.; McGrath, J. A.; Gleeson, M. J.; Hodgson, S. V.; Poulsom, R.; Rustin, P.; Tomlinson, I. P. *Hum. Mol. Genet.* **2005**, *14*, 2231−2239.

(26) Mullen, A. R.; Wheaton, W. W.; Jin, E. S.; Chen, P.-H.; Sullivan, L. B.; Cheng, T.; Yang, Y.; Linehan, W. M.; Chandel, N. S.; DeBerardinis, R. J. *Nature* **2012**, *481*, 385−388.

(27) Schumacker, P. T. *Cancer Cell* **2006**, *10*, 175−176.

(28) Sullivan, L. B.; Martinez-Garcia, E.; Nguyen, H.; Mullen, A. R.; Dufour, E.; Sudarshan, S.; Licht, J. D.; Deberardinis, R. J.; Chandel, N. S. *Mol. Cell* **2013**, *51*, 236−248.

(29) Fan, J.; Ye, J.; Kamphorst, J. J.; Shlomi, T.; Thompson, C. B.; Rabinowitz, J. D. *Nature* **2014**, *510*, 298−302.

DOI: 10.1021/ja5101257
J. Am. Chem. Soc. 2015, 137, 564−567